The electrochemical CO_2 reduction performance of Cu-Au nanoparticles with core/shell structures

Wei-I Liu (劉魏溢)[1], Kuan-Wen Wang (王冠文)[1*]
[1] Department of Materials Science and Engineering, National Central University, Taoyuan, Taiwan.
kuanwen.wang@gmail.com

Abstract

The electrochemical carbon dioxide reduction reaction (CO_2RR) has attracted a significant interest recently, as it is a possible reaction for storage of renewable energy and elimination of harmful CO_2. Controlling the compositions and structures of catalysts are the effective methods to increase catalytic selectivity and activity for CO_2RR. In this study, carbon-supported CuAu nanoparticles (NPs) with Cu core and Au shell structure were synthesized by colloidal method. The NPs composition and shell thickness were adjusted to evaluate their impacts on CO_2 to CO electrocatalytic conversion performance. NPs with a Cu/Au ratio of 8:2 and Au shell thickness of 3 nm showed the best efficiency for conversion of CO_2 to CO with a 94% CO faradaic efficiency at -0.8V (vs. RHE) as well as a high noble metal mass activity of -439 A g_{Au}^{-1}. These results, supported by extended x-ray absorption fine structure (EXAFS), indicate that the high mass activity and CO faradaic efficiency of Cu_8Au_2 NPs are due to the optimized Au and Cu intermixed layer under Au shell.

Keywords –
CO_2 reduction reaction (CO_2RR), faradaic efficiency (FE), core-shell nanoparticles (NPs), mass activity (MA)

1. Introduction

Energy and environment issues are the greatest challenges which human beings are facing in this era [1]. Although tremendous efforts have been done to develop renewables energy source [2-5], CO_2 emission from non-renewables fossil fuels are still a problem. An attractive option to solve this problem is the electrochemical reduction of CO_2 into useful intermediates or fuels such as formic acid, carbon monoxide, hydrocarbons, and alcohols [6]. Gold (Au) represents the high selectivity for the formation of CO from CO_2 [7], which broadly applied in industrial chemical manufacturing as a gas precursor [8]. However, the high cost of Au remains the primary limiting factor, which prevents its widespread application in CO_2 reduction reaction (CO_2RR).

In recent years, many Au-based catalysts have been extensively investigated for CO_2RR by tuning the catalytic properties of size [9], shapes [10] and compositions [11-13] in order to improve the performance and decrease the cost. For this reason, we use Cu-Au bimetallic nanoparticles with core-shell structure to study their CO_2RR. Trough controlling the Cu/Au ratios, the performance of catalyst was enhanced while simultaneously reducing the cost compared to pure Au.

2. Experiments

2.1 Preparation of the catalysts

Carbon-supported Cu_xAu_{10-x} NPs with metal loading of 30 wt. % and Cu/Au atomic ratio of 9/1, 8/2, and 7/3 were synthesized by the oleylamine method and named as Cu_9Au_1, Cu_8Au_2, and Cu_7Au_3 NPs, respectively

2.2 Characterization of the catalysts

The structure of catalysts was analyzed by X-ray absorption spectroscopy (XAS). XAS data was recorded at the Cu k-edge (8979 eV) and Au L_3-edge (11918 eV) at the BL17C beamline at the National Synchrotron Radiation Research Center (NSRRC).

All electrochemical measurements were performed in our customized electrochemical setup. A platinum wire and Ag/AgCl (Radiometer Analytical, 3M KCl) were used as counter and reference electrode, respectively. Both compartments were filled with electrolyte (0.1 M $KHCO_3$) and purged continuously with CO_2 (pH 6.8) at a flow rate of 40 sccm (mL min^{-1}) for at least 20 min controlled by mass flow controllers (MFCs). During constant potential electrolysis (1h), effluent gas from the working compartment went through the sampling loop of six-port valve system for a gas chromatograph (GC, Agilent 6890) for product analysis. Samples for GC were collected at 10 min intervals and the separated gas products were analyzed by pulsed discharge helium ionization detector (PDHID)..

3. Results and discussion

XAS is used to probe the structures of CuAu NPs. Absorption spectra at the Au L_3-edge and Cu K-edge are collected for Cu_9Au_1, Cu_8Au_2, and Cu_7Au_3 NPs/C. Figure 1 summarizes the Fourier transformed extended X-ray absorption fine structure spectra (FT-EXAFS) with model fitting curves of experimental CuAu NPs at Au L_3-edge XAS. In Figure 1 (a), the radial peak across 2.0 to 3.1 Å is the typical feature of X-ray interference to the Au-Au bond in the metallic phase. It is noted that the radial peak of Cu_9Au_1 in Figure 1 (b) is shifted to the left hand side as compared to that of Au-Au in Au foil. The absence of typical Au interference (the small satellite peak at 2.25 Å) and the presence of a Gaussian type radial peak (B) with an insignificant tail (2.6 to 3.0 Å, denoted by C) are typical characteristics for the formation of CuAu intermix layer. When Au contents are higher than 10% (i.e., Cu_8Au_2 and Cu_7Au_3), the suppression of peak B and the enhancement of peak C evidence the decrease in the extent of CuAu intermix and preferential formation of Au-Au cluster. The proposed structure evolutions are

further confirmed by FT-EXAFS analysis at Cu K-edge (Figure 2). In Figure 2(a), the radial peak from 1.9 to 2.8 Å is the contribution of the metallic Cu-Cu bond to X-ray interference in Cu foil. For experimental NPs, regardless of the composition differences, the shape of radial peaks remain unchanged, suggesting the absence of local atomic intermix of Au around Cu atoms. Moreover, a substantial increase of radial peak intensity is observed when Au content is increased from 10 to 30 at%, confirming again the decrease in the local structure disorder.

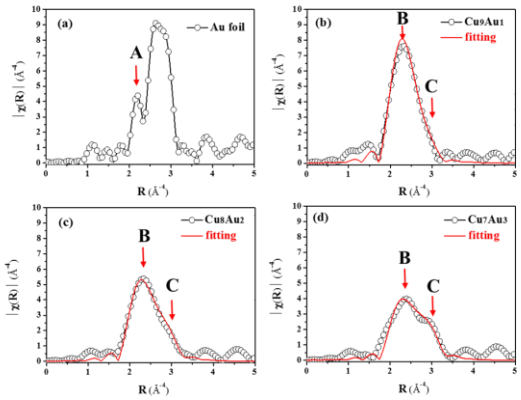

Figure 1 FT-EXAFS spectra of the Au foil and various CuAu catalysts for the Au L_3 edge.

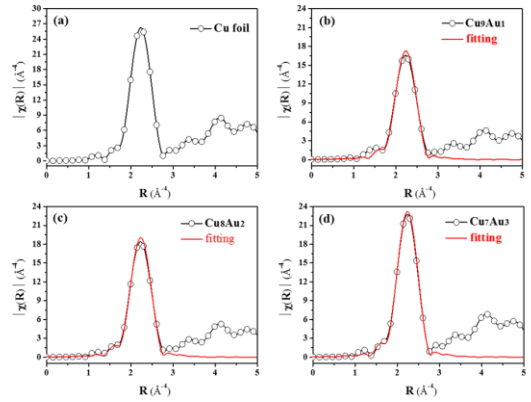

Figure 2 FT-EXAFS spectra of the Cu foil and CuAu catalysts for the Cu K-edge.

CO_2RR performance tests are analyzed in our customized electrochemical setup coupled with gas chromatography, CO_2 saturated 0.1 M $KHCO_3$ aqueous solution was employed as electrolyte. Linear sweep voltammetry results (Figure 3a) suggest that the overpotential of Cu_7Au_3 NPs is the best among all binary catalysts. On-line micro gas chromatography is responsible for products detection where CO and H_2 are major products. In Figure 3 (b) and (c), Cu_8Au_2 achieves maximum CO faradaic efficiency of 94% and exhibits -439 A g_{Au}^{-1} CO mass activity at -0.8V (vs. RHE), far exceeding -156 A g_{Au}^{-1} of Au and -122 A g_{Au}^{-1} of Cu_9Au_1. In Figure 3 (d), the stability test of Cu_8Au_2 and Au is performed at -0.8V (vs. RHE) in 0.1M $KHCO_3$ aqueous solution. A total current density and CO faradaic efficiency of Cu_8Au_2 remain around -8.5 mA/cm^2 and 90% in 3 hours, respectively while Au NPs deactivate quickly within 3 h with a decay of 36% (from 90% to 57%) in the CO faradaic efficiency, suggesting the Cu_8Au_2 NPs are promising CO_2RR catalysts.

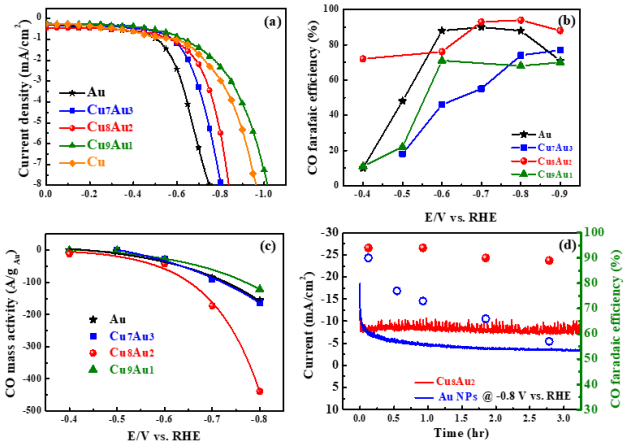

Figure 3 CO_2RR to CO performance of the Cu_9Au_1, Cu_8Au_2, and Cu_7Au_3. NPs (a) Linear Sweeping Voltammetry curves, (b) CO faradaic efficiency (%), (c) CO mass activity (A g_{Au}^{-1}) and (d) stability test.

4. References

[1] N. Bauer, I. Mouratiadou, G. Luderer, L. Baumstark, R. Brecha, O. Edenhofer and E. Kriegler, Climatic Change., 2013, 1–14.

[2] K. P. Kuhl, T. Hatsukade, E. R. Cave, D. N. Abram, J. Kibsgaard, and T. F. Jaramillo, J. Am. Chem. Soc. 2014, 136, 14107-14113.

[3] B. Kumar, J. P. Brian, V. Atla, S. Kumari, K. A. Bertram, R. T. White and J. M. Spurgeon, Catal. Today. 2016, 270, 19-30.

[4] S. Hernández, M. A. Farkhondehfal, F. Sastre, M. Makkee, G. Saracco and N. Russo, Green Chem.2017, 19, 2326-2346.

[5] B. Khezri, A. C. Fisher and M. Pumera, J. Mater Chem A. 2017, 5, 8230-8246.

[6] I. Ganesh, Renew. Sustain. Energy Rev. 2016 59, 1269.

[7] Hori, Y.; Kikuchi, K.; Suzuki, S. Chem. Lett. 1985, 14, 1695−1698

[8] S. Herna´ndez, M. A. Farkhondehfal, F. Sastre, M. Makkee, G. Saracco and N. Russo, Green Chem. 2017, 19, 2326–2346.

[9] Zhu, W.; Michalsky, R.; Metin, O. n.; Lv, H.; Guo, S.; Wright, C. J.; Sun, X.; Peterson, A. A.; Sun, S. J. Am. Chem. Soc. 2013, 135, 16833-16836.

[10] W. Zhu, Y. J. Zhang, H. Zhang, H. Lv, Q. Li, R. Michalsky, A. A. Peterson, S. Sun, J. Am. Chem. Soc. 2014, 136, 16132−16135.

[11] Kim, D.; Resasco, J.; Yu, Y.; Asiri, A. M.; Yang, P. Nat. Commun. 2014, 5, 4948.

[12] Zhou, J.-H.; Lan, D.-W.; Yang, S.-S.; Guo, Y.; Yuan, K.; Dai, L.-X.; Zhang, Y.-W. Inorg. Chem. Front. 2018, 5, 1524-1532.

[13] Sun, K.; Cheng, T.; Wu, L.; Hu, Y.; Zhou, J.; Maclennan, A.; Jiang, Z.; Gao, Y.; Goddard, W. A.; Wang, Z. J. Am. Chem. Soc. 2017, 139 (44), 15608−15611.